A. Schultz von Dratzig



## Abstract

A finite element analysis of the SciFi-Nomex-sandwich panels has been carried out in order to investigate their thermo-mechanical properties. This does not include the cooling of the silicon photomultipliers but is restricted to the panels themselves. Two kinds of panels have been considered: panels with 40 mm thickness and panels with 50 mm thickness. Both versions are equipped with mats of six layers of scintillating fibers. The analyses were carried out for a series of mechanical and thermal loads which might occur during the production or installation of the detector. For both versions the stiffnesses prove to be sufficient and no critical stresses or strains are found.

## Description of the Configuration

Two models are analized one with a panel thickness of 40 mm and one with 50 mm. The layout of the SciFi panels accordingly is as follows: Referring to figure 1 the module is symmetric to the midplane through the SciF-mat and symmetric to a plane perpendicular to the this plane and across the center of the module. At the read-out side polycarbonate endpieces

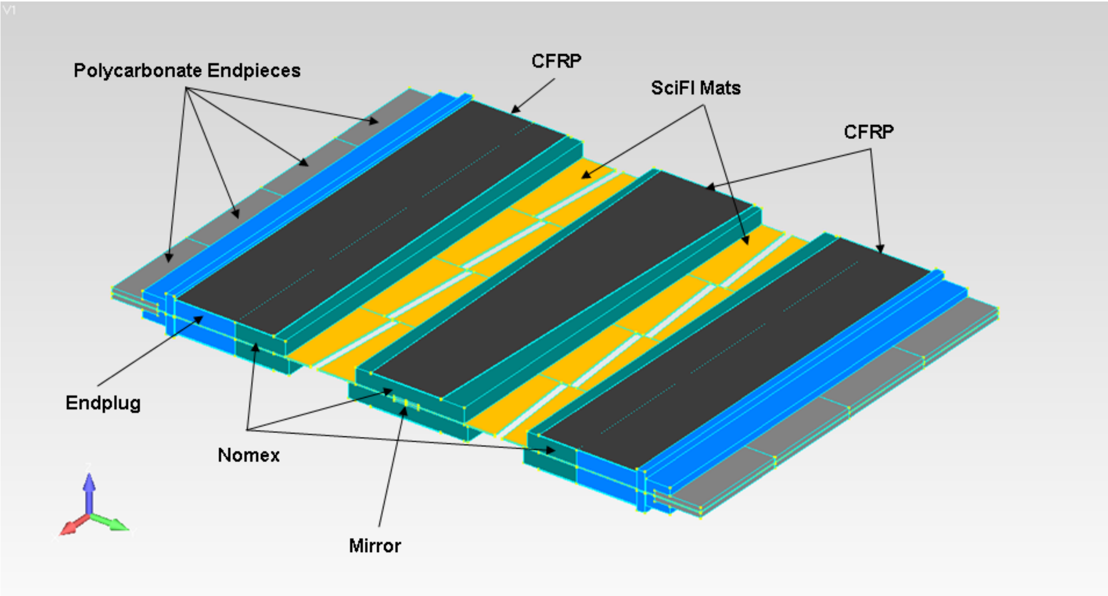


Figure 1: Geometry of the SciFi module

are glued to the SciFi-mat. At the other end polycarbonate support pieces for the mirror are attached. Four such SciFi-mats lie in parallel and another four are arranged reflected at the mirror ends leaving a gap of 2 mm for the mirrors. The module such consists of eight SciFi-mats in four columns and two rows. Aluminum end plugs run across the width of the module partly covering the endpieces and acting as a joint between the four mats. They are continued towards the mirror end by Nomex honeycombs which connect the two SciFi-mat rows. They are glued to the SciFi-mats without carbon fiber laminae in between. Onto the outer faces of the Nomex honeycombs woven carbon fiber face sheets are glued. Because the materials have very different thermal expansion coefficients a study to determine the strains has been done. In the following paragraphs a detailed description of the used FE-model is presented. The dimensions and the materials can be taken from table 1. The value in parentheses is for the 50 mm version.

Table 1: Material data of SciFi-mat material

| Object | Material | Dimension Length mm | Width mm | Thickn. mm | Quantity per Module |
|---|---|---|---|---|---|
| SciFi-mat | SciFi laminate | 2424.0 | 130.625 | 1.6 | 8 |
| Endpiece | Polycarbonate | 60.0 | 130.625 | 5.7 | 16 |
| Mirror support | Polycarbonate | 15.0 | 130.625 | 2.0 | 16 |
| End plug | Aluminum 7075-t6 | 122.0 | 528.0 | 24.2 | 4 |
| Honeycomb sandwich | Nomex | 4526.0 | 523.05 | 19.2(24.20) | 2 |
| CFRP | CFRP laminate | 4686.0 | 523.05 | 0.27 | 2 |

## 1. Mechanical Properties of the SciFi-Mat

The SciFi-mat is considered as being an unidirectional lamina of Polystyrene fibers in an epoxy matrix. In order to determine the mechanical properties the method of Composite Cylinder Assemblage (CCA) together with the so called three phase model [1–5] are used. In a CCA model, one assumes the fibers are circular in cross-section and spread in a periodic arrangement. Then the composite can be considered to be made of repeating elements called the representative volume elements. Since the CCA model only gives upper and lower limits for the transverse Young's modulus, the latter is determined with the three-phase model. The calculated mechanical and thermal data are summarized in tables 2 and 3. A compilation of the relevant formulae can be found in appendix A. A very good introduction to this theory can be found in the book of Autar K. Kaw[6].

[1] Hashin, Z., Theory of fiber reinforced materials, NASA tech. rep. contract no: NAS1-8818, November 1970.
[2] Hashin, Z. and Rosen, B.W., 1964, The elastic moduli of fiber reinforced materials, ASME J. Appl. Mech., 31, 223, 1964.
[3] Hashin, Z., Analysis of composite materials — a survey, ASME J. Appl. Mech., 50, 481, 1983.
[4] Knott, T.W. and Herakovich, C.T., Effect of fiber orthotropy on effective composite properties, J. Composite Mater., 25, 732, 1991.
[5] Christensen, R.M., Solutions for effective shear properties in three phase sphere and cylinder models, J. Mech. Phys. Solids, 27, 315, 1979.
[6] Autar K. Kaw, Mechanics of composite materials, CRC Press, 1997.

Table 2: Material data of SciFi-mat material

| Material | Quantity | Magnitude | Unit |
|---|---|---|---|
| Polystyrene | Elastic modulus $E_{PS}$ | 3300.0 | MPa |
| | Poisson const. $\nu_{PS}$ | 0.32 | |
| | Shear modulus $G_{PS}$ | 1400.0 | MPa |
| | CTE $\alpha_{PS}$ | $120.0 \times 10^{-6}$ | $K^{-1}$ |
| | Thermal conductivity $k_{PS}$ | $1.4 \times 10^{-4}$ | W/mm K |
| Epoxy resin | Elastic modulus $E_{EP}$ | 4000.0 | MPa |
| | Poisson const. $\nu_{EP}$ | 0.35 | |
| | Shear mdulus $G_{EP}$ | 1481.0 | MPa |
| | CTE $\alpha_{EP}$ | $55.0 \times 10^{-6}$ | $K^{-1}$ |
| | Thermal conductivity $k_{EP}$ | $9.0 \times 10^{-4}$ | W/mm K |

Table 3: Material data of 6 layer SciFi-mat lamina

| Quantity | Magnitude | Unit |
|---|---|---|
| Fiber volume fraction | 0.7 | |
| Elastic modulus $E_l$ | 3510.8 | MPa |
| Elastic modulus $E_t$ | 3680.5 | MPa |
| Shear modulus $G_{12}$ | 1423.8 | MPa |
| Shear modulus $G_{23}$ | 1423.7 | MPa |
| Poisson const. $\nu_{12}$ | 0.330 | |
| Poisson const. $\nu_{23}$ | 0.293 | |
| CTE $\alpha_1$ | $97.8 \times 10^{-6}$ | $K^{-1}$ |
| CTE $\alpha_2$ | $100.9 \times 10^{-6}$ | $K^{-1}$ |
| Thermal conductivity $k_1$ | $3.68 \times 10^{-4}$ | W/mm K |
| Thermal conductivity $k_2$ | $2.91 \times 10^{-4}$ | W/mm K |

## 2. Mechanical Properties of the Nomex Honeycomb

There is almost no information of the mechanical parameters of Nomex material. The only values I could find out are the two out-of-plane shear moduli of the honeycomb (Hexcel catalogue) and a range of values for the elastic modulus of the Nomex itself (between 1800.0 MPa and 5000.0 MPA). A workaround consists in making a FE model of the hexagonal cell and submit it to unit displacements in the 3 coordinate directions. The details of this method are compiled in appendix B. The result is summarized in tables 4 and 5.

Table 4: Material data of Nomex

| Quantity | Magnitude | Unit |
|---|---|---|
| Elastic modulus $E$ | 4175.0 | MPa |
| Shear modulus $G$ | 1569.5 | MPa |
| Poisson const. $\nu$ | 0.33 | |
| CTE $\alpha_{\mathrm{Nom}}$ | $20.0 \times 10^{-6}$ | $\mathrm{K}^{-1}$ |
| Therm. conductivity $k_{\mathrm{Nom}}$ | $1.3 \times 10^{-4}$ | W/mm K |

Table 5: Material data of Nomex honeycomb ECA-32-4.8

| Quantity | Magnitude | Unit |
|---|---|---|
| Elastic modulus $E_1$ | 0.0671 | MPa |
| Elastic modulus $E_2$ | 0.0671 | MPa |
| Elastic modulus $E_3$ | 118.3 | MPa |
| Shear modulus $G_{12}$ | 0.025 | MPa |
| Shear modulus $G_{13}$ | 25.0 | MPa |
| Shear modulus $G_{23}$ | 16.7 | MPa |
| Poisson const. $\nu_{12}$ | 0.999 | |
| Poisson const. $\nu_{21}$ | 0.999 | |
| Poisson const. $\nu_{13}$ | $1.9 \times 10^{-4}$ | |
| Poisson const. $\nu_{31}$ | 0.33 | |
| Poisson const. $\nu_{23}$ | $1.9 \times 10^{-4}$ | |
| Poisson const. $\nu_{32}$ | 0.33 | |
| CTE $\alpha_{1,2,3}$ | $20.0 \times 10^{-6}$ | $\mathrm{K}^{-1}$ |
| Smeared therm. conductivity $k_1$ | $2.1 \times 10^{-6}$ | W/mm K |
| Smeared therm. conductivity $k_2$ | $1.4 \times 10^{-6}$ | W/mm K |
| Smeared therm. conductivity $k_3$ | $3.7 \times 10^{-6}$ | W/mm K |

# 3. Mechanical Properties of the Woven Carbon Fiber Face Sheets

In order to determine the mechanical properties of the woven CFRP a two step procedure has to be applied. In the first step the properties of the unidirectional lamina of carbon fibers in an epoxy matrix have to be evaluated and then in a second step the weave has to be accounted for. For details of the procedure see Sang-Kwan Lee, Joon-Hyung Byun, Soon Hyung Hong, Effect of fiber geometry on the elastic constants of plain woven fabric reinforced aluminum matrix composites, Materials Science and Engineering A347 (2003), 346-358. The results presented there are also applicable for epoxy matrix fabrics and are shown in the next tables 6, 7 and 8. Details are beyond the scope of this note. With these data as input for the determination of

Table 6: Input of the material data for the CFRP/EP unidirectional ply

| Material | Quantity | Magnitude | Unit |
|---|---|---|---|
| T300 | Elastic modulus $E_f$ | 230000.0 | MPa |
| | Shear modulus $G_{f12}$ | 15000.0 | MPa |
| | Poisson const. $\nu_{f12}$ | 0.2 | |
| | CTE $\alpha_f$ | $-0.7 \times 10^{-6}$ | $K^{-1}$ |
| | Therm. conductivity $k_f$ | $5.0 \times 10^{-3}$ | W/mm K |
| Epoxy | Elastic modulus $E_m$ | 4000.0 | MPa |
| | Shear modulus $G_{m23}$ | 1481.0 | MPa |
| | Poisson const. $\nu_{m12}$ | 0.35 | |
| | CTE $\alpha_m$ | $55.0 \times 10^{-6}$ | $K^{-1}$ |
| | Therm. conductivity $k_m$ | $9.0 \times 10^{-4}$ | W/mm K |

the properties of the unidirectional ply the above mentioned CCA theory gives the following results:

Table 7: CFRP/EP unidirectional ply

| Quantity | Magnitude | Unit |
|---|---|---|
| Elastic modulus $E_1$ | 94428.4 | MPa |
| Elastic modulus $E_2$ | 8524.5 | MPa |
| Shear modulus $G_{12}$ | 2927.5 | MPa |
| Shear modulus $G_{23}$ | 2824.4 | MPa |
| Poisson const. $\nu_{12}$ | 0.281 | |
| Poisson const. $\nu_{12}$ | 0.509 | |
| CTE $\alpha_1$ | $0.72 \times 10^{-6}$ | $K^{-1}$ |
| CTE $\alpha_2$ | $44.0 \times 10^{-6}$ | $K^{-1}$ |
| Therm. conductivity $k_1$ | $2.5 \times 10^{-3}$ | W/mm K |
| Therm. conductivity $k_2$ | $1.6 \times 10^{-3}$ | W/mm K |

Using these as input for the weave one finds:

Table 8: CFRP/EP woven ply

| Quantity | Magnitude | Unit |
|---|---|---|
| Elastic modulus $E_x$ | 51677.4 | MPa |
| Elastic modulus $E_y$ | 51677.4 | MPa |
| Elastic modulus $E_z$ | 8524.0 | MPa |
| Shear modulus $G_{xy}$ | 2927.5 | MPa |
| Shear modulus $G_{xz}$ | 2875.8 | MPa |
| Shear modulus $G_{yz}$ | 2875.8 | MPa |
| Poisson const. $\nu_{xy}$ | 0.154 | |
| Poisson const. $\nu_{xz}$ | 0.452 | |
| Poisson const. $\nu_{yz}$ | 1.620 | |
| CTE $\alpha_1$ | $\approx 0.7 \times 10^{-6}$ | $K^{-1}$ |
| CTE $\alpha_2$ | $\approx 0.7 \times 10^{-6}$ | $K^{-1}$ |
| Therm. conductivity $k_1$ | $2.5 \times 10^{-3}$ | W/mm K |
| Therm. conductivity $k_2$ | $2.5 \times 10^{-3}$ | W/mm K |

# 4. Preparation of the FE Simulation

Because the SciFi-panel is not subject to bending loads the SciFi-panel will be modeled with laminate elements and solid elements for the SciFi-mat and the two Nomex volumes. The property of the SciFi solid elements are taken from the laminate properties of the SciFi-mat coated with glue on both sides (80 µm for the casting and additional 70 µm for the bonding to the honeycomb on each side) and two identical laminates for the CFRP woven face sheets coated on one side with 70 µm glue. The laminate properties are evaluated using the classical laminate theory (CLT). The following table summarizes the properties of the laminates.
As can be seen from the numbers there is no need to include the anisotropic properties of the laminates in the simulation, instead the laminates are taken to be isotropic. This is valid since the forces that act on the panels are all directed in the main directions of the laminates. The Nomex honeycomb is modeled as orthotropic material.

Table 9: Results for the laminates

| Material | Quantity | Magnitude | Unit |
|---|---|---|---|
| SciFi laminate | Elastic modulus $E_x$ | 3595.4 | MPa |
| | Elastic modulus $E_y$ | 3735.6 | MPa |
| | Shear modulus $G_{xy}$ | 1433.7 | MPa |
| | Poisson const. $\nu_{xy}$ | 0.333 | |
| | Poisson const. $\nu_{yx}$ | 0.346 | |
| | CTE $\alpha_f$ | $\approx 89.3 \times 10^{-6}$ | $K^{-1}$ |
| | CTE $\alpha_f$ | $\approx 92.4 \times 10^{-6}$ | $K^{-1}$ |
| | Therm. conductivity $k_1$ | $4.6 \times 10^{-4}$ | W/mm K |
| | Therm. conductivity $k_2$ | $4.0 \times 10^{-4}$ | W/mm K |
| Face sheet laminates | Elastic modulus $E_m$ | 39360.7 | MPa |
| | Elastic modulus $E_m$ | 39360.7 | MPa |
| | Shear modulus $G_{m23}$ | 2552.5 | MPa |
| | Poisson const. $\nu_{m12}$ | 0.160 | |
| | Poisson const. $\nu_{m12}$ | 0.160 | |
| | CTE $\alpha_m$ | $\approx 4.46 \times 10^{-6}$ | $K^{-1}$ |
| | CTE $\alpha_m$ | $\approx 4.46 \times 10^{-6}$ | $K^{-1}$ |
| | Therm. conductivity $k_1$ | $2.1 \times 10^{-3}$ | W/mm K |
| | Therm. conductivity $k_2$ | $2.1 \times 10^{-3}$ | W/mm K |

# 5. FE Model

The FE model itself is very simple. From bottom to top: a layer of CFRP laminate which also covers the 80 mm part of the Al end plug, a layer of Nomex honeycomb, where at the ends the Nomex is replaced by 15 mm long polycarbonate blocks as mirror support, four SciFi-mats 2424 mm in length with a spacing of 0.2 mm, and again Nomex with polycarbonate blocks and a CFRP layer. In the center the SciFi has a gap of 2 mm in between the SciFi-mats and the mirror supports. The read out ends have polycarbonate endpieces and Al end plugs. The dimensions are listed in table 1. All solids are modeled with hex-elements and the CFRP laminates as shells (according to the above statement). The module panel is simply supported. Both thicknesses 40 mm and 50 mm are considered.

## Mechanical Stiffness

A line load of 10 N in total is applied across the center. The panel deflects (fig. 2) by 4.49 mm (3.09 mm). Under own weight the panel sags (fig. 3) 29.6 mm (21.98 mm). The stiffness seems to be sufficient. (A panel made from Aluminum with the same geometry but with the mass of our SciFi-panel would sag ≈ 16 mm.) The torsional stiffness is investigated by supporting the panel on one side only in the corner. The free corner (fig. 4) sags by 9.9 mm (7.85 mm). Another measure for the stiffness are the eigenfrequencies. The first eigenfrequency is very low as expected (fig. 6) and lies at 3.3 Hz (3.86 Hz). In case in the pit is an air draft the effect of wind load is also been checked: with Beaufort 2 (i.e. an areal load of 3.9 N/m$^2$) the panel is pushed away by 2.7 mm (1.86 mm) (fig. 5). In no case the von-Mises stress exceeds 12 MPa.

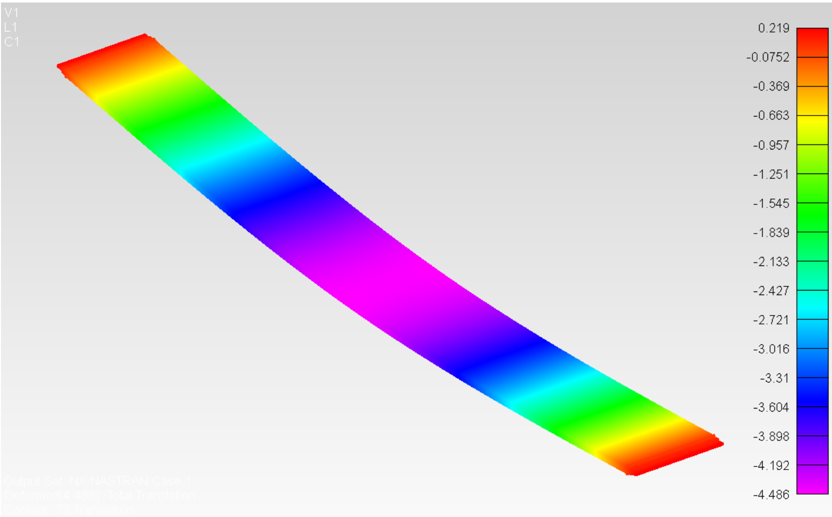


Figure 2: Deformation of the panel through a line load of 10 N. Max deflection 4.49 mm (3.09 mm)

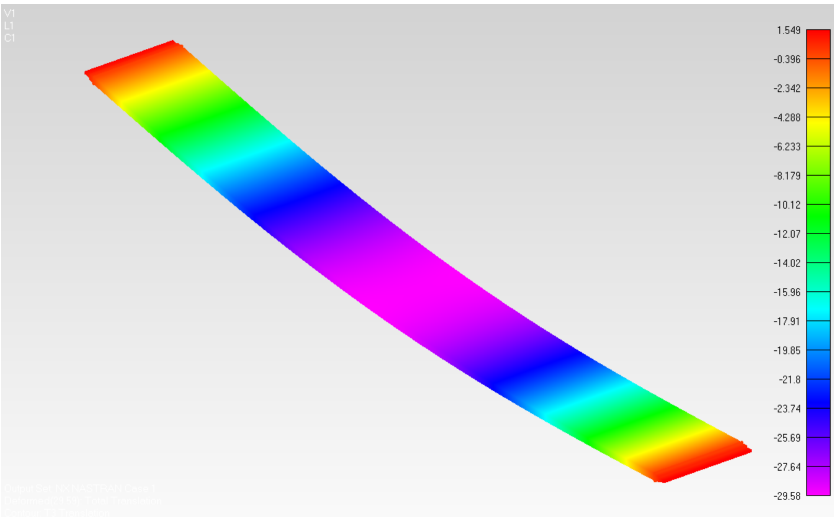


Figure 3: Deformation of the panel through own weight. Max deflection 29.6 mm (21.98 mm)

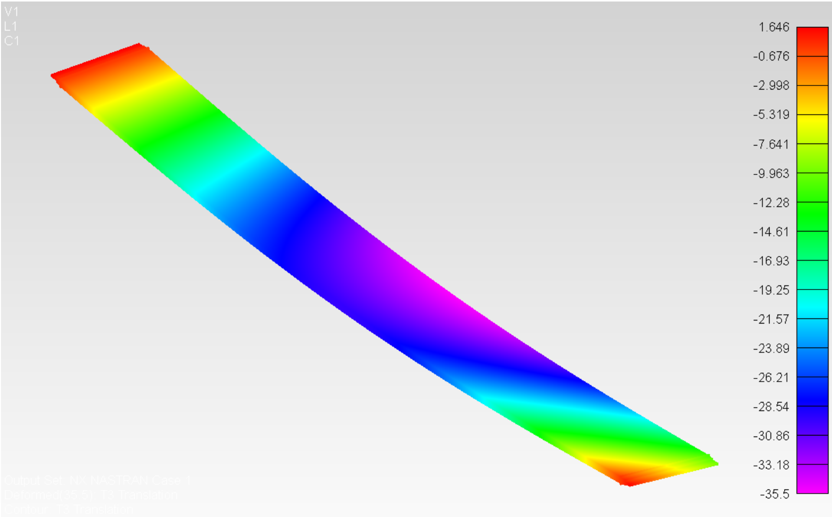


Figure 4: Deformation of the panel through own weight, support in lower right corner removed. Max deflection there 9.9 mm (7.85 mm)

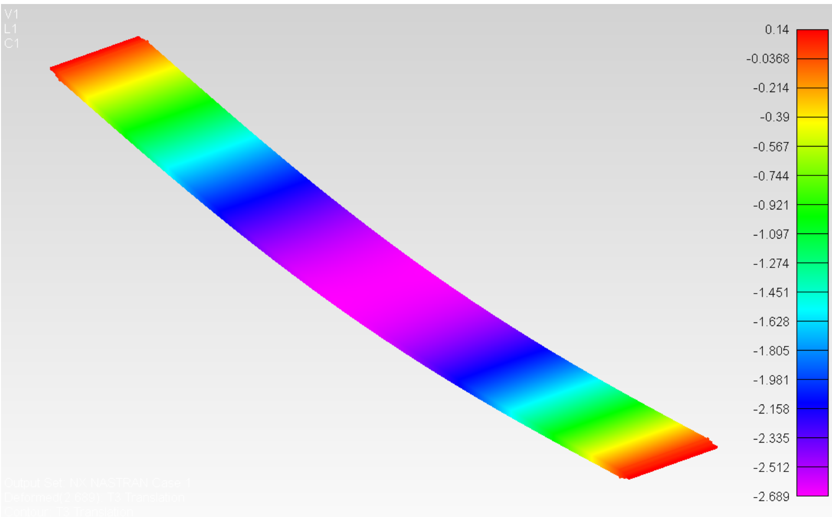


Figure 5: Deformation of the panel through air draft (Beaufort 2). Max deflection 2.7 mm (1.86 mm)

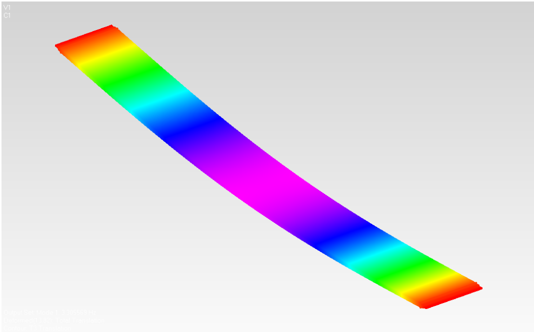

First eigenfrequency 3.3 Hz (3.86 Hz)

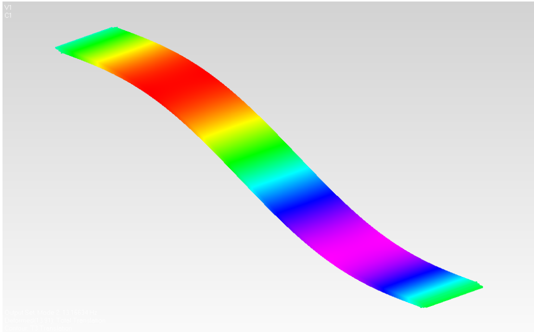

Second eigenfrequency 13.2 Hz (15.34 Hz)

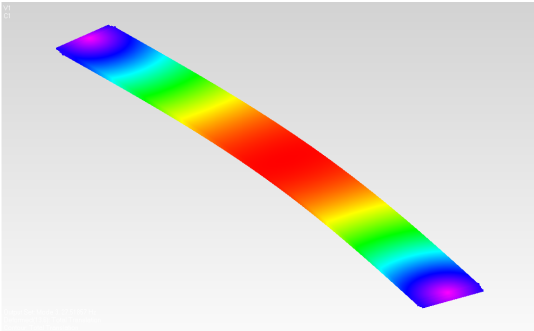

Third eigenfrequency 27.5 Hz (33.34 Hz)

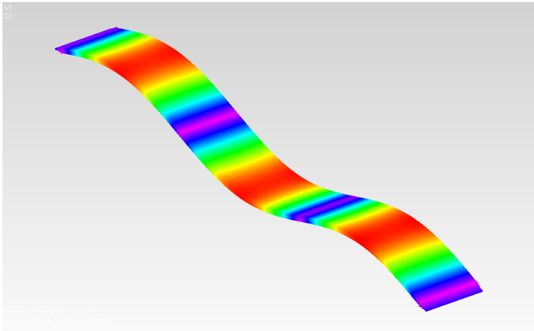

Forth eigenfrequency 28.9 Hz (40.19 Hz)

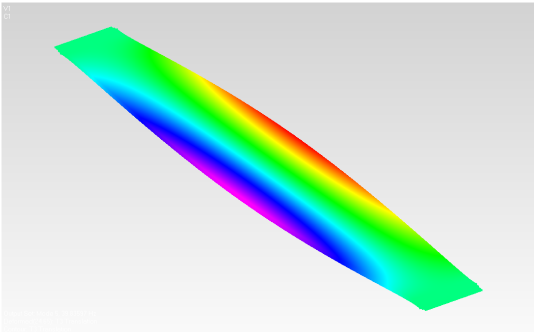

Fifth eigenfrequency 39.8 Hz (45.89 Hz)

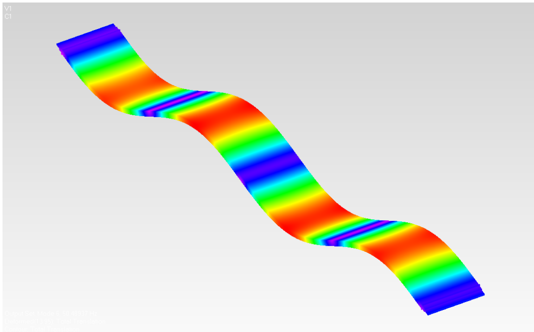

Sixth eigenfrequency 50.5 Hz (58.19 Hz)

Figure 6: First 6 eigenfrequencies of the SciFi-panel

The eigenfrequency shapes of the two versions are not always similar!

## Case All Nodes 5 °C Warmer than During the Production

All nodes are set to temperatures 5 °C higher than the assembly temperature of 20 °C. The simulation provides the resulting deformations which are shown in figures 7, 8 ,and 9. The module increases in length by 591 μm (611 μm), fig. 7. In the center a bulge of 151 μm (169 μm) in the honeycomb is visible, fig. 8. This is due to the lack of a supporting skin in the gap. We should think of a CFRP patch in the grove for the mirror supports. A much smaller effect, 50 μm (54 μm), is seen along the long edges of the panel (fig. 9). In addition the polycarbonate

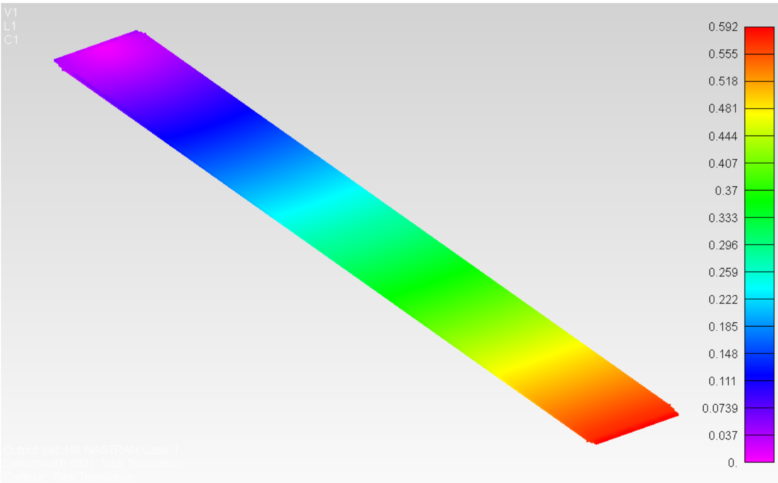


Figure 7: Deformation of the panel through a temperature difference of +5 °C

endpieces widen by a small amount of 47 μm (47 μm). The mirrors are not in danger to be

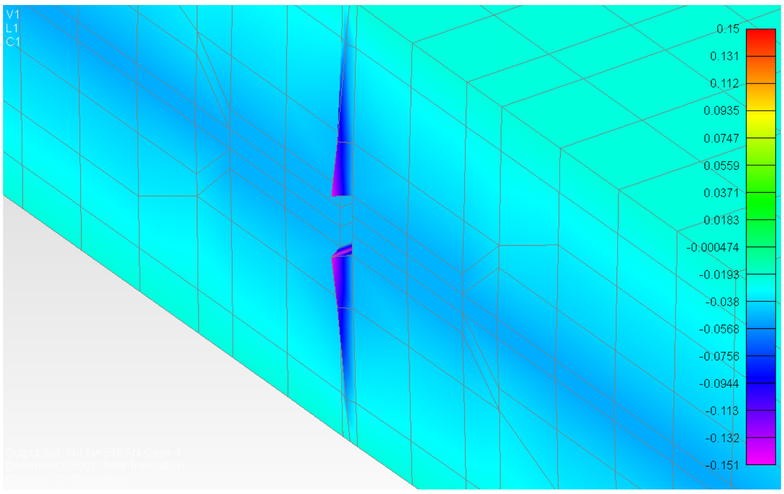


Figure 8: Detail of the deformation in the center gap of the panel through a temperature difference of +5 °C

crushed.

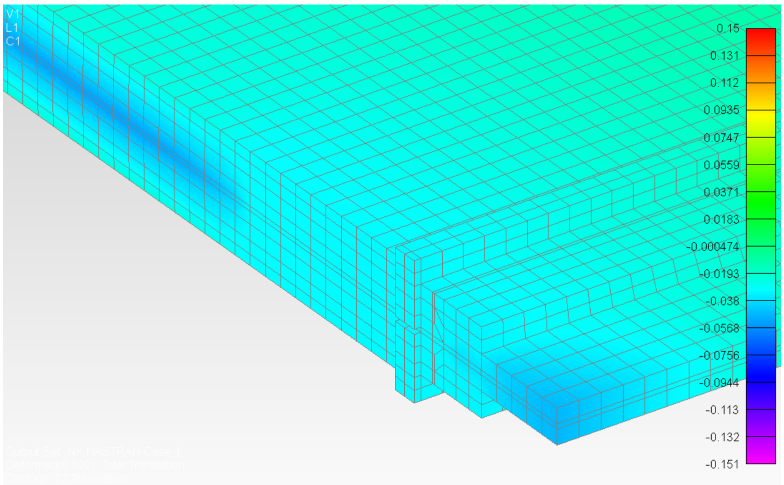


Figure 9: Detail of the deformation at the read out ends of the panel through a temperature difference of +5 °C

## Case SciFi-mat is 2 °C Warmer than the Outer Skins

No serious deformations occur. The length increases by 200 µm (204 µm), fig. 10 and a similar bulge in the center 61 µm (68 µm), fig. 11 and along the long edges 19 µm (20 µm), see fig. 12, are observable. Also the endpieces widen by 18 µm (18 µm).

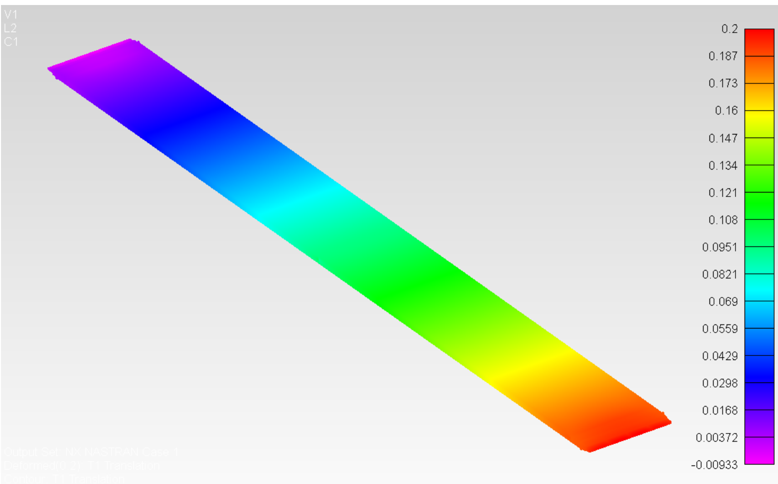


Figure 10: Increase of the length of the panel through a temperature difference of +2 °C between mat and skins

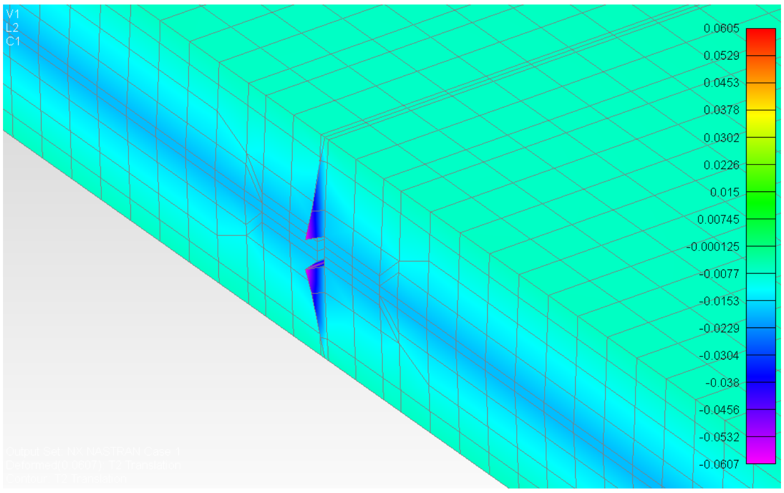


Figure 11: Detail of the deformation in the center gap of the panel through a temperature difference of +2 °C between mat and skins

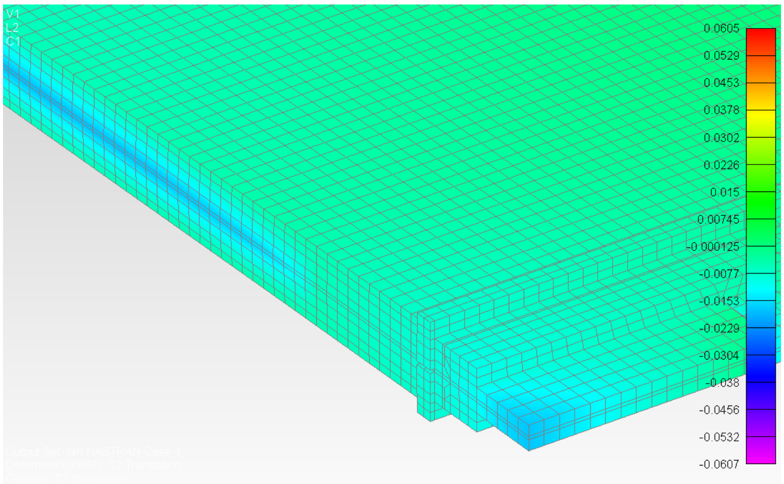


Figure 12: Detail of the deformation at the read out ends of the panel through a temperature difference of +2 °C between mat and skins

## Case One Skin 2 °C Warmer than the Opposite One

The most interesting effect is the bending of the panel through the different temperatures. It is small and in the center the »sagitta« amounts to 690 µm (574 µm). Also in this case the small bulging and the widening of the endpiece are noticeable. In the center the bulge is 30 µm

(34 µm) and alongside it is as well as the endpiece widening only 10 µm (10 µm) high.

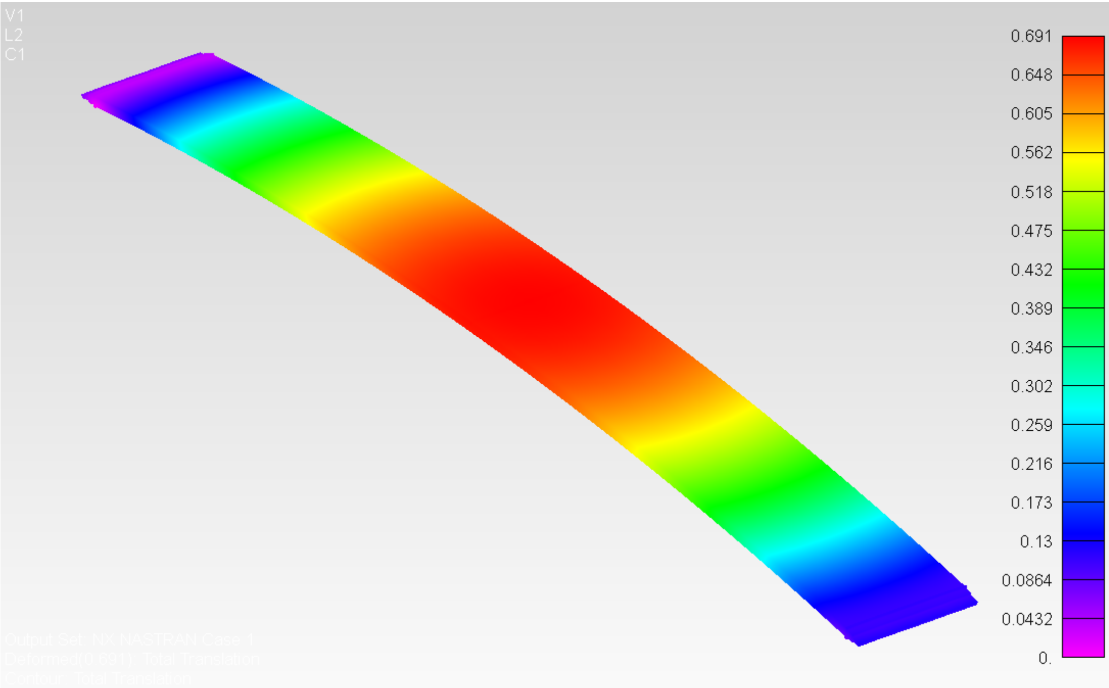


Figure 13: Deflection of the panel through a temperature difference of 2 °C between the two skins

## Case Half Model 5 °C warmer than During the Production

Half of the module is removed, i.e. the part of the module that lies above the midplane of the SciFi-mat is missing, the SciFi-mat however is not cut by this plane and is accorded for with the whole thickness. Because of the raised temperature the half module will bent (fig. 14) but the vacuum mould will prevent the module from arching (fig. 15). The stresses are smaller than 12 MPa. This is also true for the 50 mm version.

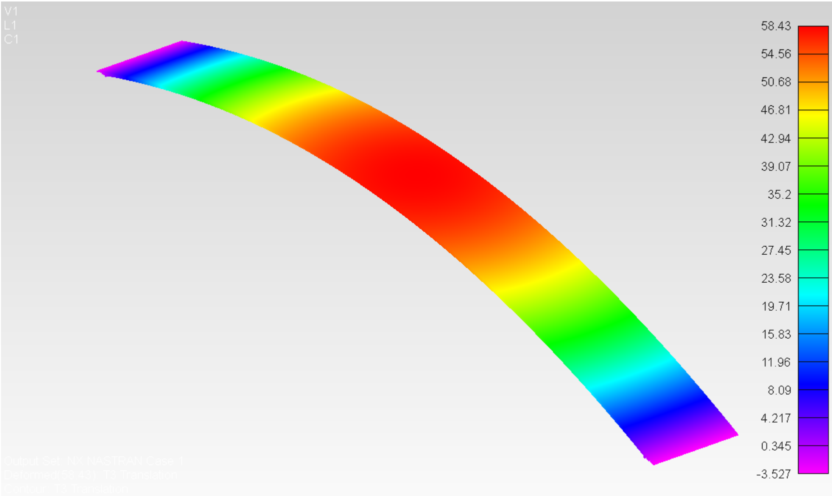


Figure 14: Half model deformation of the panel through a temperature difference of 5 °C above production temperature

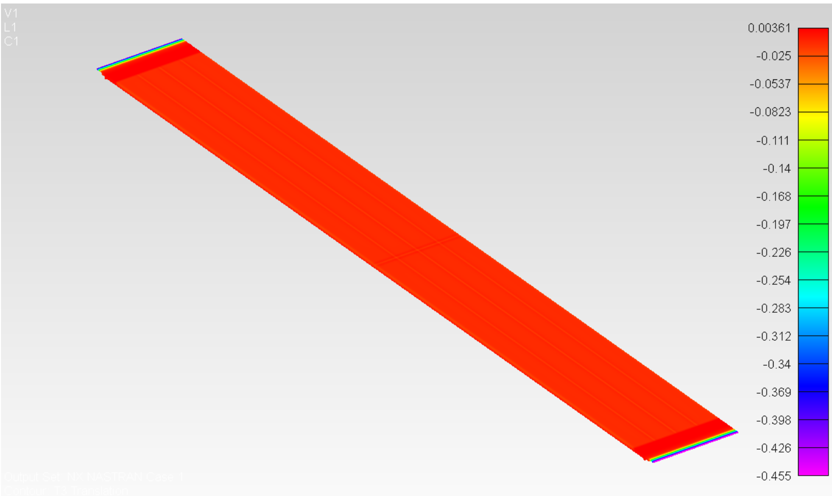


Figure 15: No deformation of the half panel in the vacuum mould

## 6. Conclusion

None of the investigated load cases shows any critical deformations or stresses. All strains are in the order of tenths of a millimeter and the stresses remain below 12 MPa. The deformations through the applied forces (own weight, air draught, torsion) are tolerable although a better rigidity would be desirable. As expected the 50 mm version is preferable as the stiffness is concerned. It has to be balanced against the radiation length difference.

# A. The CCA Model

The Composite Cylinder Assemblage (CCA) model gives simple closed form analytical expressions for the effective composite moduli $E_1$, $\nu_{12}$ and $G_{12}$, while the moduli $E_2$ and $G_{23}$ are bracketed by close bounds. Here, the UD composite cylinder consists of the inner circular fibre and the outer concentric matrix shell. The fibre and matrix are considered to be transversely isotropic. The main elastic modulus in the direction of the fibers is given by

$$\begin{aligned} E_1 = & E_f V_f + E_m(1-V_f) - \\ & - \frac{2E_m E_f V_f(\nu_f-\nu_m)^2(1-V_f)}{E_f(2\nu_m^2 V_f - \nu_m + V_f\nu_m - V_f - 1) - E_m(2\nu_f^2 V_f - \nu_f + V_f\nu_f - V_f + 1 - 2\nu_f^2)} \end{aligned} \tag{1}$$

and the major Poisson's ratio by

$$\begin{aligned} \nu_{12} = & \nu_f V_f + \nu_m(1-V_f) + \\ & + \frac{V_f V_m(\nu_f-\nu_m)(2E_f\nu_m^2 + \nu_m E_f - E_f + E_m - E_m\nu_f - 2E_m\nu_f^2)}{E_f(2\nu_m^2 V_f - \nu_m + V_f\nu_m - V_f - 1) - E_m(2\nu_f^2 V_f - \nu_f + V_f\nu_f - V_f + 1 - 2\nu_f^2)} \end{aligned} \tag{2}$$

The axial shear modulus comes out as

$$G_{12} = G_m\left[\frac{G_f(1+V_f) + G_m(1-V_f)}{G_f(1-V_f) + G_m(1+V_f)}\right] \tag{3}$$

The transverse Young's modulus is drawn from the three-phase model. A closed-form expression for this property has been proposed by Christensen and Lo (1979). This model is based upon a three-phase cylinder in which the fiber and matrix are embedded in an annulus of the equivalent homogeneous material. The full expression for the transverse modulus using this three-phase model is quite involved (see Christensen and Lo, 1979[7]). The transverse shear modulus, $G_{23}$, is given by the acceptable solution of the quadratic equation

$$A\left(\frac{G_{23}}{G_m}\right)^2 + 2B\left(\frac{G_{23}}{G_m}\right) + C = 0 \tag{4}$$

and the transverse Young's modulus by

$$E_2 = 2(1+\nu_{23})G_{23} \tag{5}$$

The factors $A$, $B$ and $C$ are given by the rather confusing equations

$$\begin{aligned} A = & 3V_f(1-V_f)^2\left(\frac{G_f}{G_m}-1\right)\left(\frac{G_f}{G_m}+\eta_f\right) + \\ & + \left[\frac{G_f}{G_m}\eta_m + \eta_f\eta_m - \left(\frac{G_f}{G_m}\eta_m - \eta_f\right)V_f^3\right]\left[V_f\eta_m\left(\frac{G_f}{G_m}-1\right) - \left(\frac{G_f}{G_m}\eta_m + 1\right)\right] \end{aligned} \tag{6}$$

[7] R.M. Christensen, K.H. Lo, Solutions for effective shear properties in three phase sphere and cylinder models, J. Mech. Phys. Solids, 27 (1979), pp. 315–330

$$\begin{aligned}B =& -3V_\mathrm{f}(1-V_\mathrm{f})^2\left(\frac{G_\mathrm{f}}{G_\mathrm{m}}-1\right)\left(\frac{G_\mathrm{f}}{G_\mathrm{m}}+\eta_\mathrm{f}\right)+\\ &+\frac{1}{2}\left[\frac{G_\mathrm{f}}{G_\mathrm{m}}\eta_\mathrm{m}+\left(\frac{G_\mathrm{f}}{G_\mathrm{m}}-1\right)V_\mathrm{f}+1\right]\left[(\eta_\mathrm{m}-1)\left(\frac{G_\mathrm{f}}{G_\mathrm{m}}+\eta_\mathrm{f}\right)-2\left(\frac{G_\mathrm{f}}{G_\mathrm{m}}\eta_\mathrm{m}-\eta_\mathrm{f}\right)V_\mathrm{f}^3\right]\\ &+\frac{V_\mathrm{f}}{2}(\eta_\mathrm{m}+1)\left(\frac{G_\mathrm{f}}{G_\mathrm{m}}-1\right)\left[\frac{G_\mathrm{f}}{G_\mathrm{m}}+\eta_\mathrm{f}+\left(\frac{G_\mathrm{f}}{G_\mathrm{m}}\eta_\mathrm{m}-\eta_\mathrm{f}\right)V_\mathrm{f}^3\right]\end{aligned} \tag{7}$$

$$\begin{aligned}C =& 3V_\mathrm{f}(1-V_\mathrm{f})^2\left(\frac{G_\mathrm{f}}{G_\mathrm{m}}-1\right)\left(\frac{G_\mathrm{f}}{G_\mathrm{m}}+\eta_\mathrm{f}\right)+\\ &+\left[\frac{G_\mathrm{f}}{G_\mathrm{m}}\eta_\mathrm{m}+\left(\frac{G_\mathrm{f}}{G_\mathrm{m}}-1\right)V_\mathrm{f}+1\right]\left[\frac{G_\mathrm{f}}{G_\mathrm{m}}+\eta_\mathrm{f}+\left(\frac{G_\mathrm{f}}{G_\mathrm{m}}\eta_\mathrm{m}-\eta_\mathrm{f}\right)V_\mathrm{f}^3\right]\end{aligned} \tag{8}$$

where

$$\eta_\mathrm{f} = 3-4\nu_\mathrm{f} \qquad \text{and} \qquad \eta_\mathrm{m} = 3-4\nu_\mathrm{m} \tag{9}$$

The transverse Poisson's ratio is given by

$$\nu_{23} = \frac{K^* - mG_{23}}{K^* + mG_{23}} \tag{10}$$

where

$$m = 1 + 4K^*\frac{\nu_{12}^2}{E_1} \tag{11}$$

In these equations the bulk modulus $K^*$ is given by

$$K^* = \frac{K_\mathrm{m}(K_\mathrm{f}+G_\mathrm{m})V_\mathrm{m} + K_\mathrm{f}(K_\mathrm{m}+G_\mathrm{m})V_\mathrm{f}}{(K_\mathrm{f}+G_\mathrm{m})V_\mathrm{m} + (K_\mathrm{m}+G_\mathrm{m})V_\mathrm{f}} \tag{12}$$

with

$$K_\mathrm{f} = \frac{E_\mathrm{f}}{2(1+\nu_\mathrm{f})(1-2\nu_\mathrm{f})} \qquad \text{and} \qquad K_\mathrm{m} = \frac{E_\mathrm{m}}{2(1+\nu_\mathrm{m})(1-2\nu_\mathrm{m})} \tag{13}$$

# B. FE Determination of Nomex Honeycomb Properties

A hexagonal cell is taken as a representative for the honeycomb core material. The forces to produce unit displacements in the 3 main directions are determined by FE models, in which the correct boundary conditions are of crucial importance. Once knowing the forces one can calculate the effective engineering constants $E_i$, $G_{ij}$ and $\nu_{ij}$, $i,j = x,y,z$[8].

$$E_i = \frac{\sigma_i}{\varepsilon_i} = \frac{F_i/A_i}{u_i/L_i} \tag{14}$$

$$\nu_{ij} = -\frac{\varepsilon_j}{\varepsilon_i} = -\frac{u_{ij}/L_j}{u_i/L_i} \tag{15}$$

$$G_{i,j} = \frac{\tau_{ij}}{\gamma_{ij}} = \frac{F_i/A_i}{u_i/L_i} \tag{16}$$

[8] The method is taken from: F. Ernesto Penado, Effective elastic properties of honeycomb core with fiber-reinforced composite cells, Open Journal of Composite Materials, 2013, 3,89-96

The $F$'s are resulting forces to produce the unit displacement in the indicated direction, the $L$'s are the cell lengths in the respective direction and the $A$'s are the projected areas of core on a plane perpendicular to the respective direction. The $u_{ij}$'s are the resulting displacements in the $j$-direction when a unit displacement is applied in the $i$-direction.
It is not necessary to model a whole hexagonal cell; when applying the correct symmetry respectively antisymmetry boundaries an eighth of a cell is sufficient shown in the figure 16.
The FE-model is shown in figure 17.

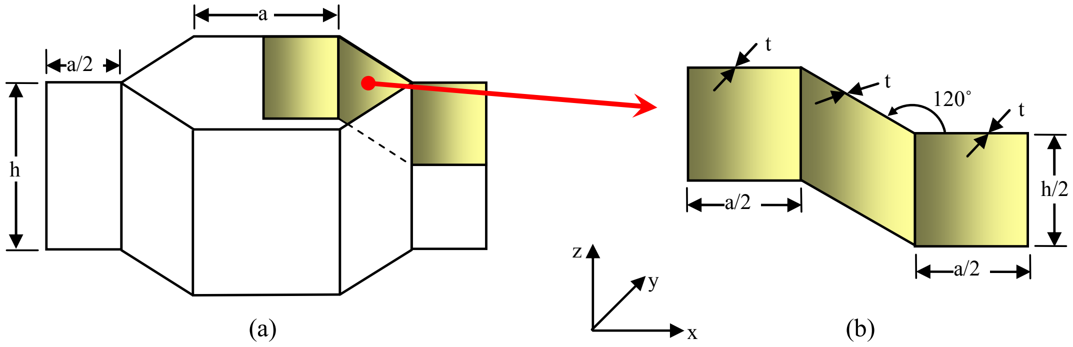


Figure 16: 1/8 segment of the unit cell

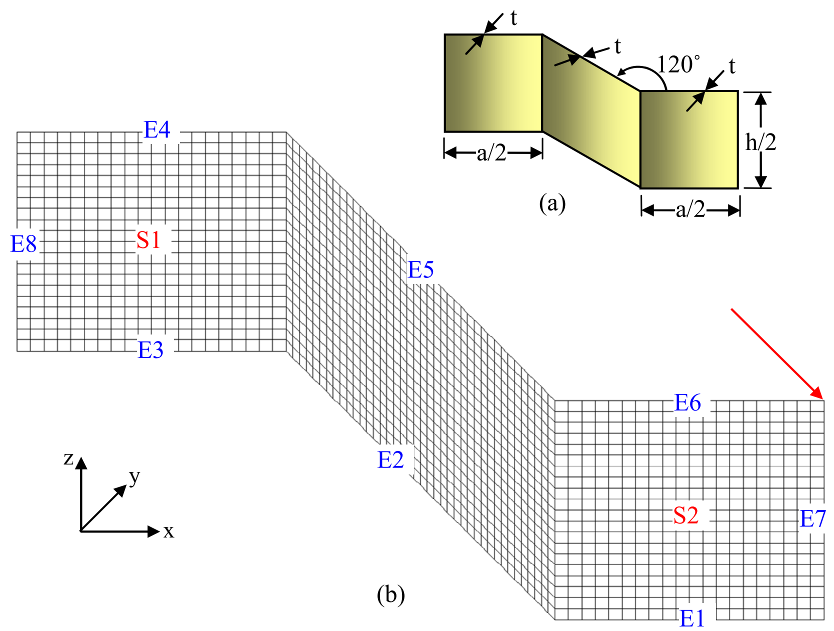


Figure 17: 1/8 segment prepared for the FE analysis

Table 10: Boundary conditions needed for the proper modeling of 1/8 segment of a unit cell
(sym: symmetry boundary, asym: anti-symmetry, cpd nds: coupled nodes, rot: rotational degrees of freedom)

| Location | $E_x, \nu_{xy}, \nu_{xz}$ | $E_y, \nu_{yz}$ | $E_y$ | $G_{xy}$ | $G_{xz}$ | $G_{yz}$ |
|---|---|---|---|---|---|---|
| E1 | sym z | sym z | sym z | asym z | asym z | asym z |
| E2 | sym z | sym z | sym z | asym z | asym z | asym z |
| E3 | sym z | sym z | sym z | asym z | asym z | asym z |
| E4 | $u_z$ cpd nds | $u_z$ cpd nds | $u_z = 1$ | free | $u_x, u_y = 0$ | $u_x, u_y = 0$ |
| E5 | $u_z$ cpd nds | $u_z$ cpd nds | $u_z = 1$ | free | $u_x, u_y = 0$ | $u_x, u_y = 0$ |
| E6 | $u_z$ cpd nds | $u_z$ cpd nds | $u_z = 1$ | free | $u_x, u_y = 0$ | $u_x, u_y = 0$ |
| E7 | $u_z = 1$ | $u_z$ cpd nds | $u_x$ cpd nds | $u_y = 1$ | $u_x, u_y = 0, u_z = 1$ | sym x |
| E8 | sym x | sym x | sym x | asym x | asym x | sym x |
| S1 | sym y | sym y | sym y | asym y | sym y | asym y |
| S2 | $u_y$ cpd nds no rot | $u_y = -1$ no rot | $u_y$ cpd nds no rot | asym y | sym y | $u_x, u_y = 0, u_z = -1$ |

In addition the following relations are valid

$$G_{xy} = G_{yx} \qquad G_{xz} = G_{zx} \qquad G_{yz} = G_{zy} \tag{17}$$

$$\nu_{yx} = \frac{E_y}{E_x}\nu_{xy} \qquad \nu_{zx} = \frac{E_z}{E_x}\nu_{xz} \qquad \nu_{zy} = \frac{E_z}{E_y}\nu_{yz} \tag{18}$$